

IMPACT OF TEMPERATURE AND EXPLOITATION TIME ON PLANE STRAIN FRACTURE TOUGHNESS, K_{Ic} , IN A WELDED JOINT

UTICAJ TEMPERATURE I VREMENA EKSPLOATACIJE NA ŽILAVOST LOMA K_{Ic} PRI RAVNOM STANJU DEFORMACIJE U ZAVARENOM SPOJU

Originalni naučni rad / Original scientific paper

UDK /UDC: 669.15'26'28-194:539.42

621.791.05:539.42

Rad primljen / Paper received: 13.12.2017

Adresa autora / Author's address:

¹⁾ University of Priština, Faculty of Technical Sciences, Kosovska Mitrovica, Serbia email: ivica.camagic@pr.ac.rs

²⁾ University of Belgrade, Innovation Centre of the Faculty of Mech. Engng., Belgrade, Serbia

³⁾ University of Belgrade, Faculty of Mech. Engng., Serbia

⁴⁾ VTI (Military Technical Institute), Belgrade, Serbia

Keywords

- low-alloyed steel
- welded joint
- crack
- plane strain fracture toughness
- critical crack length

Abstract

This paper presents the analysis of the impact of temperature and exploitation time on the tendency toward brittle fracture of welded joint constituents of new and exploited low-alloyed Cr-Mo steel A-387 Gr. B, by using fracture mechanics parameters. The exploited parent metal is a part of the reactor mantle which has been in service for over 40 years and is in the damage repair stage, i.e. in the stage where a part of the mantle is being replaced with new material. Testing of the fracture toughness at plane strain is done in order to determine critical value of stress intensity factor, K_{Ic} , i.e. evaluation of behaviour of new and exploited parent metal (PM), weld metal (WM) and heat affected zone (HAZ). Based on the testing results, the analysis of tendency to brittle fracture represents the comparison of the obtained values for characteristic areas of the welded joint and the justification of selected welding technology.

INTRODUCTION

A long-time exploitation period of a pressure vessel reactor (over 40 years) has caused damages to the reactor mantle. After a thorough inspection of the reactor structure, damaged parts are repaired, including replacement of a part of reactor mantle with newly built-in material. The pressure vessel is made of low-alloyed Cr-Mo steel A-387 Gr. B in accordance with ASTM standard. For designed operating parameters ($p = 35$ bar and $t = 537^\circ\text{C}$) the material has a tendency to decarbonise at the surface in contact with hydrogen, reducing its strength. Therefore, a comparison of new and exploited parent metal (PM) and components of welded joints (weld metal - WM, heat affected zone - HAZ) is performed, including fracture mechanics parameters of new and exploited PM, as well as welded joint components, at room and working temperature of 540°C , /1/.

Ključne reči

- niskolegirani čelik
- zavareni spoj
- prsline
- žilavost loma pri ravnoj deformaciji
- kritična dužina prsline

Izvod

Analiziran je uticaja temperature i vremena eksploatacije na sklonost ka krtom lomu konstituenata zavarenog spoja novog i eksploatisanog niskolegiraniog Cr-Mo čelika A-387 Gr. B primenom parametara mehanike loma. Eksploatisani osnovni metal je deo plašta reaktora koji je bio u eksploataciji preko 40 godina i u fazi je sanacije oštećenja, odnosno, zamene dela plašta novougrađenim materijalom. Ispitivanje žilavosti loma pri ravnoj deformaciji je rađeno u cilju određivanja kritičnog faktora intenziteta napona, K_{Ic} , odnosno, ocene ponašanja novog i eksploatisanog osnovnog metala (OM), metala šava (MŠ) i zone uticaja toplote (ZUT) sa strane novog OM i sa strane eksploatisanog OM u prisustvu greške tipa prsline. Na osnovu rezultata ispitivanja, analiza sklonosti ka krtom lomu predstavlja poređenje dobijenih vrednosti za karakteristične oblasti zavarenog spoja i opravdanost izabrane tehnologije zavarivanja.

MATERIALS FOR TESTING

Exploited PM was steel A-387 Gr. B with thickness of 102 mm, whereas the new PM is also made of steel A-387 Gr. B and thickness of 102 mm. Chemical composition and mechanical properties of the exploited and new PM according to the attest documentation are given in tab. 1 and 2, /1/.

Welding of steel sheets made of exploited and new PM was performed in two stages, according to the requirements given in the welding procedure provided by a welding specialist, and these stages include:

- root weld by E procedure, using a coated LINCOLN S1 19G electrode (AWS: E8018-B2), and
- filling by submerged arc welding (SAW) with LINCOLN LNS 150 wire and LINCOLN P230 flux, used as consumables.

The chemical composition of the LINCOLN S1 19G coated electrode, and LINCOLN LNS 150 wire, according to the attest documentation is given in Table 3, whereas their mechanical properties, also according to the attest documentation, are given elsewhere, /1/.

The butt-welded joint is made with a U-weld. The shape of the groove for welding preparation is chosen based on sheet thickness, in accordance with appropriate standards SRPS EN ISO 9692-1:2012, /2/, and SRPS EN ISO 9692-2:2008, /3/.

Table 1. Chemical composition of exploited and new PM specimens.

Specimen	% mas.							
	C	Si	Mn	P	S	Cr	Mo	Cu
E	0.15	0.31	0.56	0.007	0.006	0.89	0.47	0.027
N	0.13	0.23	0.46	0.009	0.006	0.85	0.51	0.035

Table 2. Mechanical properties of exploited and new PM specimens.

Specimen	Yield stress $R_{p0.2}$ (MPa)	Tensile strength R_m (MPa)	Elongation A (%)	Impact energy (J)
E	320	450	34.0	155
N	325	495	35.0	165

DETERMINATION OF FRACTURE TOUGHNESS IN PLANE STRAIN CONDITIONS

The impact of exploitation conditions, i.e. exploitation time and temperature on the tendency toward brittle fracture of the new and exploited PM, as well as the welded joint components (WM, HAZ) is estimated by determining the fracture toughness in plane strain conditions, that is, critical values of the stress intensity factor, K_{Ic} . Tests are conducted at room temperature of 20°C, and working temperature of 540°C.

For the purpose of determining K_{Ic} at room temperature, three-point bending specimens (SEB) are used, whose geometry is defined by standards ASTM E399, /4/, and ASTM E1820, /5/. For determining K_{Ic} at working temperature of 540°C, the modified CT tensile specimens are used, whose geometry is in accordance with BS 7448 Part 1, /6/.

Fracture toughness, K_{Ic} , is determined indirectly through critical J -integral, J_{Ic} , using elastic-plastic fracture mechanics (EPFM) defined by ASTM E813, /7/, ASTM E 1737, /8/, ASTM E1820, /5/, and BS 7448 Part 1 and 2, /6, 9/, monitoring the crack development in conditions of plasticity.

The American society for testing and materials (ASTM) has established a standard procedure for crack growth resistance curves of metallic material testing, /8/. The improvement of the standard was carried out within the framework of the European Structural Integrity Society ESIS, /10/. Some of the solutions of this standard are also adopted in this paper and refer to the determination of fitted regression line. Standards /4, 5, 7, 8, 11-13/, are regularly updated, and it is very important to make sure that the latest versions are applied.

Experiments are carried out by the testing method of single specimen successive partial unload, i.e. by single specimen permeability method, as defined by ASTM E813, /7/. The objective of the permeability method with unload is to register the size of crack development, Δa , that occurs during testing. Testing of specimens taken from the sample

with the fatigue crack tip in the exploited and new PM, WM, and HAZ from both the exploited and new side, is performed at 20°C room temperature, and at 540°C working temperature, by electromechanical testing machine.

When testing at room temperature, the specimen is equipped with COD extensometer for registering crack tip opening displacement. This was not the case when testing was conducted at high temperatures. Namely, due to the fact that extensometer fails to operate at high temperatures, the crack tip opening is registered with the inductive transducer, with previously registered calibration curves of ratio values obtained on extensometer and inductive transducer.

The bending load or the yield stress, depending on the type of the specimen we tested, is introduced at low speed, and in this case the speed of load introduction was 1 mm/min. The load is introduced with occasional unloads from the moments of significant plastic deformation or fracture of the specimen, i.e. getting out from the scope of the extensometer or inductive transducer. During this time, the A/D converter collected data of load and crack tip opening displacement.

Based on the obtained data, a J - Δa curve is constructed in which the regression line is constructed according to ASTM E1152, /12/. From the obtained regression line, the critical J -integral, J_{Ic} , is obtained. Knowing the value of critical, J_{Ic} , integral, the value of critical stress intensity factor or plane strain fracture toughness, K_{Ic} , can be calculated using the dependence:

$$K_{Ic} = \sqrt{\frac{J_{Ic} E}{1 - \nu^2}} \quad (1)$$

Calculated values of critical stress intensity factor, K_{Ic} , are given in Table 3 for notched specimens in new PM, and in Table 4 for notched specimens in exploited PM, tested at 20°C and 540°C, /1/.

It is important to point out that when calculating plane strain fracture toughness, K_{Ic} , one value of elastic modulus is used at room temperature (210 GPa) and the other value for increased temperatures (approximately 160 GPa at 540°C). By applying the basic formula of fracture mechanics:

$$K_{Ic} = \sigma \sqrt{\pi a_c} \quad (2)$$

and by introducing the values of conventional yield stress, $R_{p0.2} = \sigma$, /1, 14/, the approximate values for critical crack length, a_c , can be calculated.

Characteristic diagrams F - δ and J - Δa for specimen from sample of new PM are given in Fig. 1 for specimen marked PM-1-1n, tested at room temperature, and in Fig. 2 for specimen marked PM-2-1n, tested at 540°C, /1/.

Diagrams F - δ , and J - Δa for specimens of exploited PM WM and HAZ from the side of new PM and HAZ from the side of exploited PM, tested at room- and working temperature, due to the scope of the paper are not presented, /1/.

The influence of testing temperature on the value of critical stress intensity factor, K_{Ic} , for specimens taken from the new and exploited PM is graphically illustrated in Fig. 3, and the impact of temperature on the critical crack length, a_c , is graphically illustrated in Fig. 4, /1/.

Table 3. Values of K_{Ic} for notched specimens in new PM.

Specimen mark	Test temperature (°C)	Critical J-integral J_{Ic} (kJ/m ²)	Critical stress intensity factor K_{Ic} (MPa m ^{1/2})	Critical crack length a_c (mm)
PM-1-1n	20	60.1	117.8	38.5
PM-1-2n		63.9	121.4	40.8
PM-1-3n		58.6	116.3	37.5
PM-2-1n	540	43.2	87.2	40.0
PM-2-2n		44.7	88.7	41.4
PM-2-3n		45.3	89.2	41.9

Table 4. Values of K_{Ic} for notched specimens in exploited PM.

Specimen mark	Test temperature (°C)	Critical J-integral J_{Ic} (kJ/m ²)	Critical stress intensity factor K_{Ic} (MPa m ^{1/2})	Critical crack length a_c (mm)
PM-1-1e	20	47,8	105,0	41,7
PM-1-2e		42,1	98,6	36,8
PM-1-3e		40,7	96,9	35,6
PM-2-1e	540	24,5	65,6	30,8
PM-2-2e		22,7	63,2	28,6
PM-2-3e		21,8	61,9	27,4

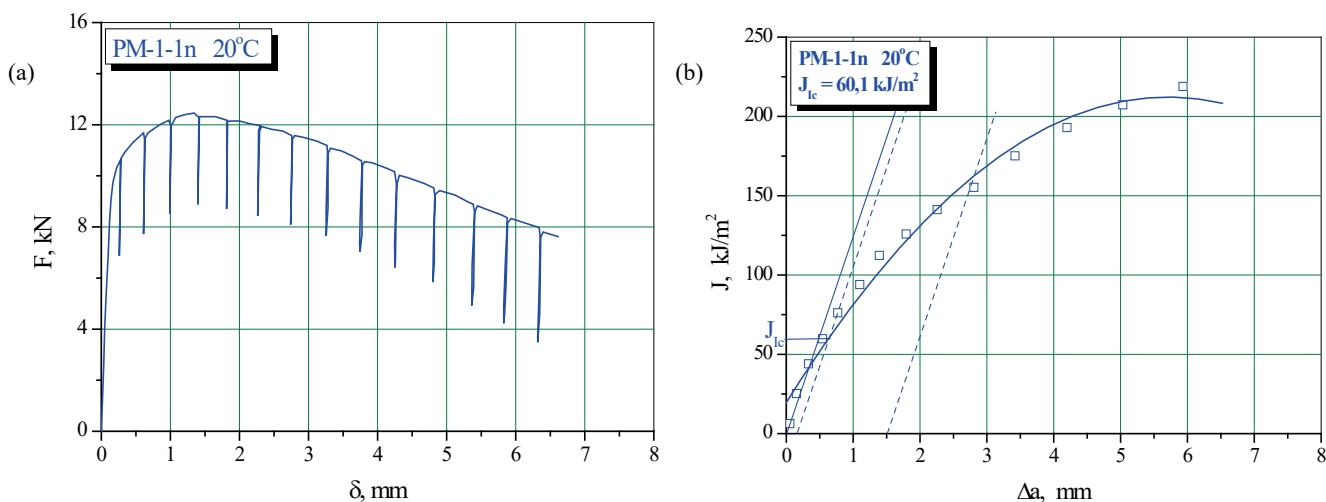


Figure 1. Diagrams $F-\delta$ (a), and $J-\Delta a$ (b) of the specimen PM-1-1n.

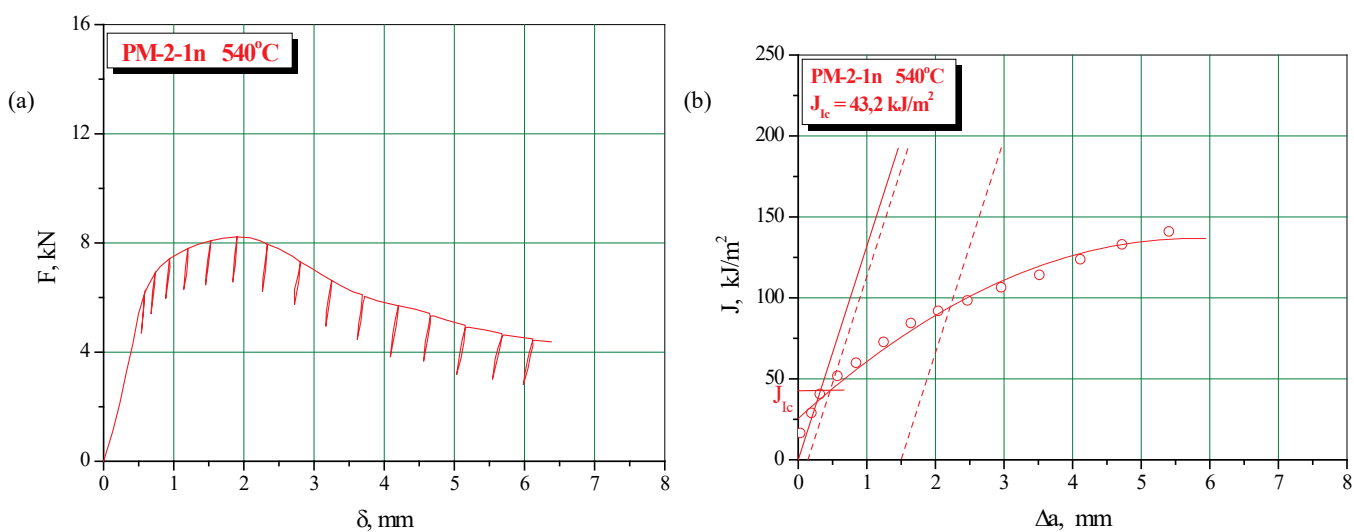


Figure 2. Diagrams $F-\delta$ (a), and $J-\Delta a$ (b) of the specimen PM-2-1n.

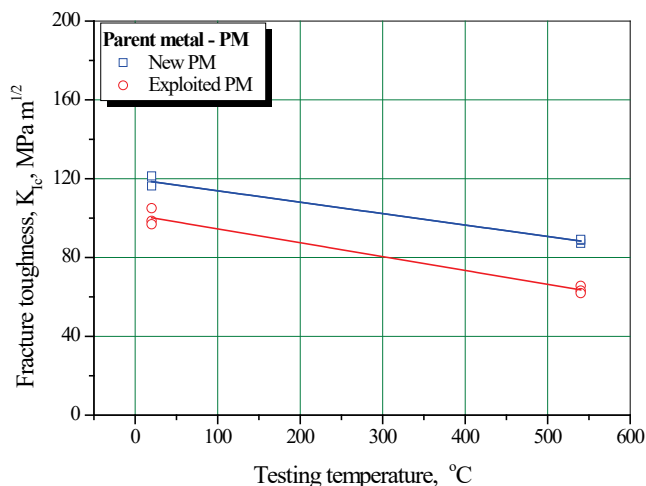


Figure 3. Change in value of K_{Ic} vs. test temperature for PM.

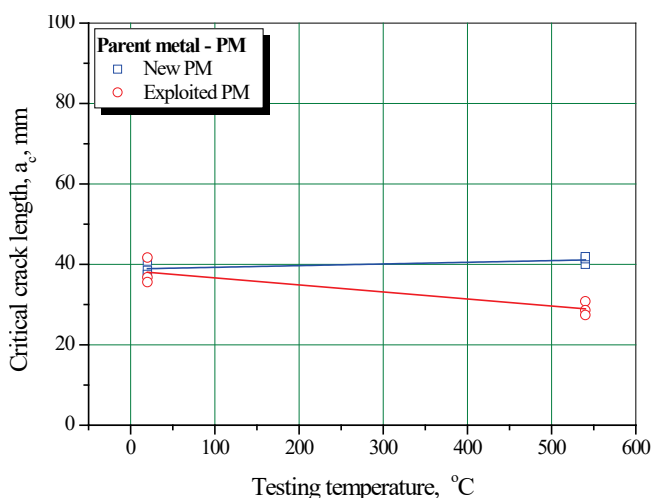


Figure 4. Change in value of a_c vs. test temperature for PM.

Calculated values of critical stress intensity factor, K_{Ic} , and critical crack length, a_c , are given in Table 5 for notched specimens in WM, tested at room temperature of 20°C and working temperature of 540°C, /1/.

Table 5. Values of K_{Ic} for notched WM specimens.

Specimen mark	Test temp. (°C)	Critical J-integral J_{Ic} (kJ/m ²)	Critical stress intensity factor K_{Ic} (MPa m ^{1/2})	Critical crack length a_c (mm)
WM-1-1	20	72.8	129.6	20.2
WM-1-2		74.3	130.9	20.7
WM-1-3		71.1	128.1	19.8
WM-2-1	540	50.2	93.9	17.4
WM-2-2		52.6	96.2	18.2
WM-2-3		48.4	92.2	16.8

Impact of test temperature on the value of critical stress intensity factor, K_{Ic} , for specimens notched in WM is graphically illustrated in Fig. 5, and the impact of test temperature on the value of critical crack length, a_c , is graphically illustrated in Fig. 6, /1/.

Calculated values of critical stress intensity factor, K_{Ic} , and critical crack length, a_c , are given in Table 6 for specimens notched in HAZ from the side of new PM, and

in Table 7 for specimens notched in HAZ from the side of exploited PM, tested at room temperature of 20°C and working temperature of 540°C, /1/.

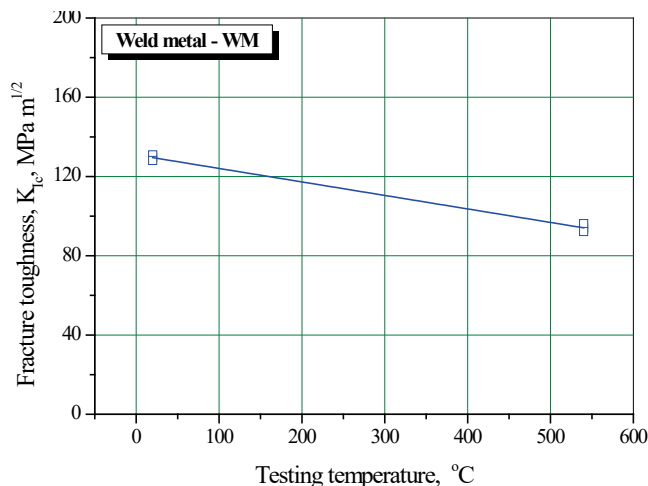


Figure 5. Change in value of K_{Ic} vs. test temperature for WM. 1

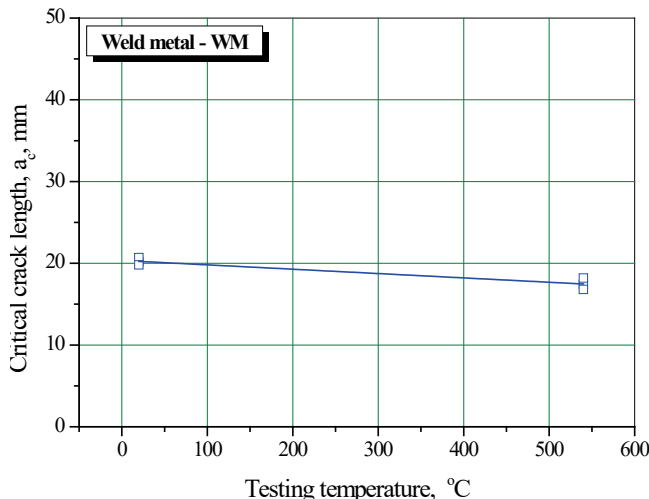


Figure 6. Change in value of a_c depending on the testing temperature at WM

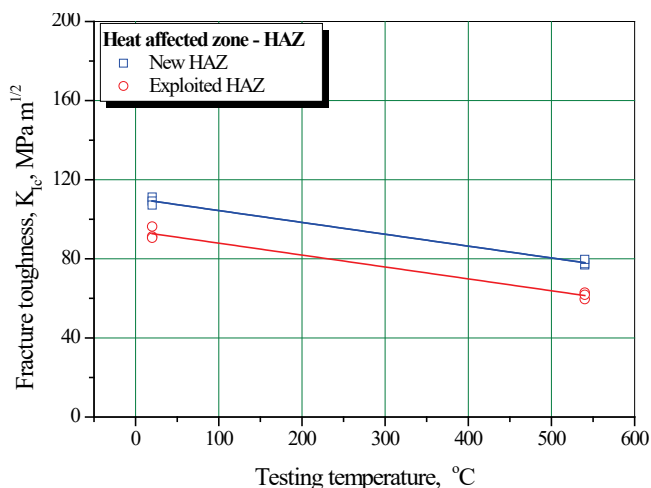
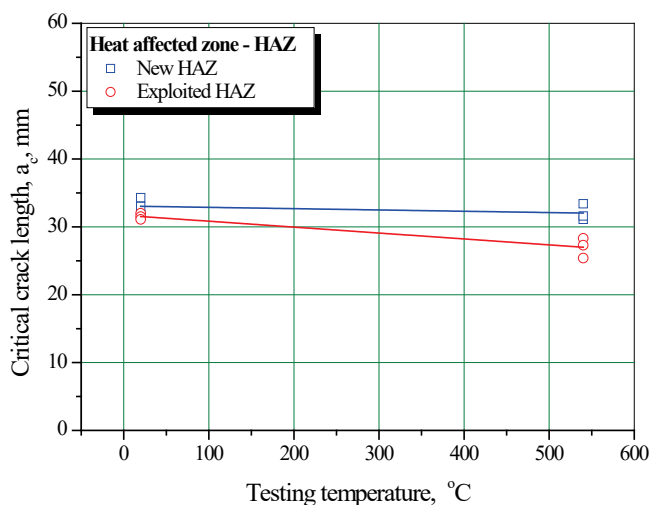
Table 6. Values of K_{Ic} for specimens notched in new HAZ.

Specimen mark	Test temp. (°C)	Critical J-integral J_{Ic} (kJ/m ²)	Critical stress intensity factor K_{Ic} (MPa m ^{1/2})	Critical crack length a_c (mm)
HAZ-1-1n	20	53.6	111.2	34.3
HAZ-1-2n		51.7	109.2	33.0
HAZ-1-3n		49.8	107.2	31.8
HAZ-2-1n	540	33.6	76.9	31.1
HAZ-2-2n		34.2	77.5	31.6
HAZ-2-3n		36.1	79.7	33.4

The impact of testing temperature on the values of critical stress intensity factor, K_{Ic} , for specimens notched in HAZ on the side of new and exploited PM is graphically illustrated in Fig. 7, and the impact of testing temperature on the values of critical crack length, a_c , is graphically illustrated in Fig. 8, /1/.

Table 7. Values of K_{Ic} for specimens notched in exploited HAZ.

Specimen mark	Test temp. (°C)	Critical J-integral J_{Ic} (kJ/m ²)	Critical stress intensity factor K_{Ic} (MPa m ^{1/2})	Critical crack length a_c (mm)
HAZ-1-1e	20	42.4	96.3	32.0
HAZ-1-2e		36.1	91.3	31.5
HAZ-1-3e		35.6	90.6	31.1
HAZ-2-1e	540	20.2	59.6	25.4
HAZ-2-2e		22.5	62.9	28.3
HAZ-2-3e		21.7	61.8	27.3

Figure 7. Change in value of K_{Ic} vs. test temperature for HAZ.Figure 8. Change in value of a_c vs. test temperature for HAZ.

DISCUSSION

Based on the results of testing specimens from the new and exploited PM, it can be seen that with the increase of testing temperature there is a decrease in the value of critical integral, J_{Ic} , that is, fracture toughness, K_{Ic} .

Fracture toughness values, K_{Ic} , of specimens taken from the new PM, Table 5, range from 118 MPa·m^{1/2} obtained at 20°C and decrease to 88 MPa·m^{1/2} at 540°C. Likewise, the fracture toughness values, K_{Ic} , of specimens taken from exploited PM, Table 6, range from 100 MPa·m^{1/2} obtained at 20°C, and also decrease to 64 MPa·m^{1/2} at 540°C, /1/.

Obtained values of critical crack length, a_c , Fig. 4, for new PM are almost unchanged when it comes to room or working temperature. This is expected, because for calculating critical crack length, a_c , the real values of yield stress obtained from tensile testing are used. However, exploitation weakening of the PM has led to the fact that the value of a_c for specimens from exploited PM decreases by about 24% and is about 29 mm, /1/.

Based on the results of testing notched specimens for WM, it can be seen that with the increase of testing temperature, there is a decrease in the value of critical J_{Ic} integral, that is, fracture toughness, K_{Ic} . Fracture toughness values, K_{Ic} , of notched specimens for WM, Table 7, range from 130 MPa·m^{1/2} obtained at 20°C to 94 MPa·m^{1/2} obtained by testing at 540°C, /1/.

Obtained values of critical crack length, a_c , in relation to the yield stress level are quite low, and range from 20.2 mm at room temperature, and decrease to 17.5 mm at 540°C. However, if values of critical crack length, a_c , in relation to the yield stress of new and exploited OM are calculated, they are significantly higher and indicate good resistance to brittle fracture in WM, /1/.

Based on the results of testing specimens from HAZ, it can be seen that with the increase of testing temperature there is a decrease in the value of critical J_{Ic} , that is, fracture toughness, K_{Ic} . The value of critical crack length, a_c , also decreases.

Fracture toughness values, K_{Ic} , of specimens notched in HAZ from the side of new PM, Table 8, range from 109 MPa·m^{1/2} obtained at 20°C, and decrease to 78 MPa·m^{1/2} obtained at 540°C, /1/. By testing specimens notched in HAZ from the side of exploited PM, Table 9, poorer values of fracture toughness, K_{Ic} , are obtained. Namely, the value of plane strain fracture toughness, K_{Ic} , ranges from 93 MPa·m^{1/2} obtained at 20°C, and decreases to 61 MPa·m^{1/2} obtained at 540°C, /1/.

The values of critical crack length, a_c , Fig. 8, at HAZ from the side of the new PM are slightly changed when it comes to room or working temperature. However, exploitation weakening of the PM has led to the decrease of a_c . In specimens notched in the HAZ from the side of exploited PM and at 540°C $a_c = 27$ mm, /1/.

CONCLUSIONS

The weakest resistance to crack propagation at static action of force, that is, the lowest value, K_{Ic} , is for specimens notched in HAZ, and the best resistance to crack propagation is for specimens notched in WM. The character of the curves exclusively changes depending on: testing temperature; placement of notches; and exploitation time. By analysing the obtained curves, we see the almost identical character dependence of individual curves in each group, except that the difference between the specimens is in the values of maximal force, F_{max} , which directly depends on fatigue crack length, a , /1/.

Exploitation time significantly impacts the resistance to crack propagation, which generally should be related to the weakening of mechanical exploitation properties of the used material in relation to the new material. It can be seen

that exploitation period of 40 years has an impact on the values of plane strain fracture toughness, K_{Ic} , and for exploited PM and HAZ from the side of exploited PM it decreases, Tables 6 and 9. The resistance to crack propagation in specimens from exploited PM and HAZ from the side of exploited PM is approximately 20% lower than in specimens from the samples of new PM, and HAZ from the side of the new PM, /1/.

The results of fracture mechanics parameters (K_{Ic} , J_{Ic} and a_c) indicate two things. First, the tendency toward brittle fracture under static loading conditions is the lowest for specimens notched in WM and PM, and is the highest for specimens notched in HAZ, i.e. HAZ in the concrete case has the worst resistance to brittle fracture. Second, the results of the exploited material indicate a significant difference compared to the new material.

Testing results and their analysis have justified the selected welding technology for the replacement of a part of the reactor mantle.

ACKNOWLEDGEMENT

Parts of this research is supported by the Ministry of Education, Science and Technological Development of the Republic of Serbia through Mathematical Institute SANU Belgrade project grant OI 174001 - *Dynamics of hybrid systems with complex structures*.

REFERENCES

1. Čamagić, I., *Investigation of the effects of exploitation conditions on the structural life and integrity assessment of pressure vessels for high temperatures* (in Serbian), doctoral thesis, University of Priština, Faculty of Tech. Sciences, Kosovska Mitrovica, 2013.
2. SRPS EN ISO 9692-1:2012, Welding and allied processes - Recommendations for joint preparation - Part 1: Manual metal-arc welding, gas-shielded metal-arc welding, gas welding, TIG welding and beam welding of steels (ISO 9692-1:2003), 2012.
3. SRPS EN ISO 9692-2:2008, Welding and allied processes - Joint preparation - Part 2: Submerged arc welding of steels (ISO 9692-2:1998), 2008.
4. ASTM E399-89, Standard Test Method for Plane-Strain Fracture Toughness of Metallic Materials, Annual Book of ASTM Standards, Vol. 03.01. p. 522. 1986.
5. ASTM E 1820-99a, Standard Test Method for Measurement of Fracture Toughness, Annual Book of ASTM Standards, Vol. 03.01, 1999.
6. BS 7448-Part 1, Fracture mechanics toughness tests-Method for determination of K_{Ic} critical CTOD and critical J values of metallic materials, BSI, 1991.
7. ASTM E813-89, Standard Test Method for J_{Ic} , A Measure of Fracture Toughness, Annual Book of ASTM Standards, Vol. 03.01. p. 651, 1993.
8. ASTM E 1737-96, Standard Test Method for J Integral Characterization of Fracture Toughness, Annual Book of ASTM Standards, Vol.03.01., 1996.
9. BS 7448-Part 2, Fracture mechanics toughness tests - Methods for determination of K_{Ic} , critical CTOD and critical J values of welds in metallic materials, BBI, 1997.
10. 'ESIS Procedure for Determining the Fracture Behaviour of Materials', European Structural Integrity Society ESIS P2-92, 1992.
11. BS 5762-DD 19, Standard Test Method for Crack Opening Displacement, London, 1976.
12. ASTM E1152-91, Standard Test Method for Determining J-R Curve, Annual Book of ASTM Standards, Vol. 03.01. p. 724, 1995.
13. ASTM E 1290-89, Standard Test Method for Crack-Tip Opening Displacement (CTOD) Fracture Toughness Measurement, Annual Book of ASTM Standards, Vol. 03.01, 1993.
14. Čamagić, I., Burzić, Z., A. Sedmak, et al., *Temperature effect on a low-alloyed steel welded joints tensile properties*, Proc. 3rd IIW South-East Euro. Welding Cong.: 'Welding & Joining Technol. for a Sustainable Devel. & Environment', Editura Politehnica, 2015, Timisoara, Romania, pp.77-81. ISBN 978-606-554-955-5.

© 2017 The Author. Structural Integrity and Life, Published by DIVK (The Society for Structural Integrity and Life 'Prof. Dr Stojan Sedmak') (<http://divk.inovacionicentar.rs/ivk/home.html>). This is an open access article distributed under the terms and conditions of the [Creative Commons Attribution-NonCommercial-NoDerivatives 4.0 International License](#)